

Nuclear spin relaxation in solid state defect quantum bits via electron-phonon coupling in their optical excited state

Gergő Thiering¹ and Adam Gali^{1,2,3}

¹*HUN-REN Wigner Research Centre for Physics, P.O. Box 49, H-1525 Budapest, Hungary*

²*Department of Atomic Physics, Institute of Physics,
Budapest University of Technology and Economics,
Műgyetem rakpart 3., H-1111 Budapest, Hungary*

³*MTA-WFK Lendület “Momentum” Semiconductor Nanostructures Research Group, P.O. Box 49, H-1525 Budapest, Hungary*

(Dated: March 1, 2024)

Optically accessible solid state defect spins are primary platform for quantum information processing where tight control of the electron spin and ancilla nuclear spins is pivotal for the operation. We demonstrate on the exemplary nitrogen-vacancy (NV) color center in diamond by means of a combined group theory and density functional theory study that spin-phonon relaxation rate of the nitrogen nuclear spin is with several orders of magnitude enhanced by the strong electron-phonon coupling in the optical excited state of the defect. The mechanism is common to other solid state defect spins sharing similar optical excited states with that of the NV center.

Solid state defect quantum bits are versatile platform for quantum information processing [1–6]. The most studied defect quantum bit is the nitrogen-vacancy (NV) color center in diamond where the electron spin state can be initialized and readout via spin-selective non-radiative decay from its optical excited state [7, 8]. The hyperfine interaction between the electron spin and the nuclear spins of the nitrogen and proximate ¹³C atoms makes it possible to control the nuclear spins that can be harnessed in quantum sensing, quantum communication and quantum computation applications [9–20]. It is a common assumption that the relaxation time of the nuclear spins is orders of magnitude longer than that of the electron spin in diamond [21–29] and can be employed as quantum memories. This assumption is based on the weak phonon-nuclear spin interaction in the electronic ground state of the NV center in diamond. However, the NV qubits are typically read out by optical excitation. Understanding the properties of the nuclear spins of the defect qubits requires to monitor the evolution of the nuclear spin’s state throughout the optical cycles used to readout the quantum bit.

In this study, we report the theory of the spin-lattice relaxation of the nuclear spins of NV center in diamond. We develop and implement a theory to compute the dynamical spin-related parameters at *ab initio* level that is relevant in the electronic excited state. We show that the spin-lattice relaxation of the nuclear spins is enhanced by several orders of magnitude in the optical excited state caused by the strong electron-phonon coupling. The discovered mechanism is general for the system and can be applied to other optically read solid state defect quantum bits which possess orbitally degeneracy in their excited state which is entangled and mediated by strong electron-phonon coupling.

We applied *ab initio* density functional theory (DFT) calculations to calculate the spin parameters in the optical excited state that are not directly observable. We ap-

plied Heyd-Scuzeria-Ernzerhof (HSE) hybrid functional with HSE06 parameters [30] to obtain the magnetic parameters [31–35] and the adiabatic potential energy surface in the excited state with Δ SCF method [36] except for the zero-field splitting tensor that was calculated with Perdew-Burke-Ernzerhof (PBE) functional [37] as implemented by Martijn Marsman to the VASP code [38–40]. We note that the strong electron-phonon coupling as parameterized by Jahn-Teller theory [41–43] were already reported and is used in this study [43]. The calculations were carried out in a 512-atom diamond supercell with Γ -point sampling of the Brillouin-zone. We applied a plane wave cutoff of 370 eV with projector augmented wave method [44].

The NV center in diamond consists of a nitrogen atom substituting a carbon atom adjacent to a vacancy where the defect accepts an electron from the lattice that establishes the negative charge state with a ground state $S = 1$ spin. The defect has C_{3v} symmetry and their electronic wavefunctions are labeled by the single group (*orbital*) and double group (*orbital with spin*) notations [45, 46]. The ground state is an orbital singlet $|^3A_2\rangle$ whereas the optical excited state is an orbital doublet $|^3E\rangle$. The orbital doublet is a Jahn-Teller (JT) system [42], in other words, strong electron-phonon coupled system which significantly interferes with the spin-orbit interaction [43]. In adiabatic potential energy surface (APES) DFT calculations, the JT system is manifested as breaking the symmetry to C_{1h} symmetry that we can refer to as low-symmetry configuration. On the other hand, the dynamics of the electron and the phonons is in the femtosecond regime [47, 48], thus the JT effect is dynamic and an effective C_{3v} symmetry is observed in the pulsed optically detected magnetic resonance experiments. As a consequence, the $|^3E\rangle$ wavefunctions are polaronic dressed states [8, 43] but we simply label them with the usual notations as $|E_{1,2}\rangle$ ($m_S = \pm 1$), $|E_{x,y}\rangle$ ($m_S = 0$), $|A_1\rangle$ and $|A_2\rangle$ ($m_S = \pm 1$).

These levels are separated due to electron spin-spin interaction (D -tensor) and spin-orbit interaction (λ). If strain is present then the degenerate $|E_{1,2}\rangle$ and $|E_{x,y}\rangle$ states split whereas the $m_S = \pm 1$ levels may further split in the presence of external constant magnetic field which all finally set the final energy spacing between these states (Fig. 1). The $|^3A_2\rangle$ ground state fine structure is much simpler: the $|A_1\rangle$ ($m_S = 0$) and the E ($m_S = \pm 1$) levels are split by the magnetic spin-spin interaction of electrons where strain may split the E spin doublet further. The $|^3E\rangle$ level structure simplifies to that of $|^3A_2\rangle$ at $T > 20$ K temperatures because the thermal averaging of orbital degrees of freedom. We keep the low-temperature level structure of $|^3E\rangle$ in the discussion which can reveal the complex physics between the nuclear spins and phonons. We write the six individual eigenstates within the $|^3E\rangle$ manifold as follows

$$\begin{aligned} |A_1\rangle &= \frac{1}{\sqrt{2}}(|E_-^{\uparrow\uparrow}\rangle - |E_+^{\downarrow\downarrow}\rangle), & |A_2\rangle &= \frac{1}{\sqrt{2}}(|E_-^{\uparrow\uparrow}\rangle + |E_+^{\downarrow\downarrow}\rangle), \\ |E_x\rangle &= \frac{1}{\sqrt{2}}(|E_-^0\rangle + |E_+^0\rangle), & |E_y\rangle &= \frac{1}{\sqrt{2}}(|E_-^0\rangle - |E_+^0\rangle), \\ |E_1\rangle &= \frac{1}{\sqrt{2}}(|E_-^{\downarrow\downarrow}\rangle - |E_+^{\uparrow\uparrow}\rangle), & |E_2\rangle &= \frac{1}{\sqrt{2}}(|E_-^{\downarrow\downarrow}\rangle + |E_+^{\uparrow\uparrow}\rangle), \end{aligned} \quad (1)$$

where $|E_{m_L}^{m_S}\rangle$ subscript and superscript symbols depict the orbital moment and spin, respectively.

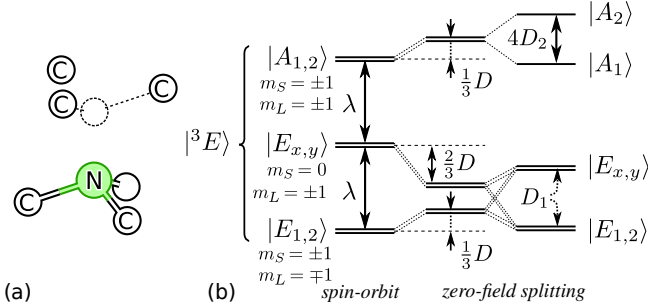


FIG. 1. NV center in diamond. (a) Structure. (b) Levels in the 3E excited state for temperatures below 15 K. The λ , D , D_2 interactions of Eqs. (2) and (4) are diagonal in the basis spanned by Eq. (1), thus the energy shift for these parameters is depicted. We note that D_1 mixes the $m_S = 0$ spin projection with $m_S = \pm 1$ ones. However, this effect is almost negligible, thus we still use $|E_{x,y}\rangle$ and $|E_{1,2}\rangle$ as pure eigenstates.

We consider the ^{14}N $I = 1$ nuclear spin which is

$$\begin{aligned} \hat{W} &= D_1^{(e)} \left[(\hat{S}_z \hat{S}_+ + \hat{S}_+ \hat{S}_z) \hat{\sigma}_- + (\hat{S}_z \hat{S}_- + \hat{S}_- \hat{S}_z) \hat{\sigma}_+ \right] + D_2^{(e)} \left[\hat{S}_-^2 \hat{\sigma}_- + \hat{S}_+^2 \hat{\sigma}_+ \right] + \\ &Q_1^{(e)} \left[(\hat{I}_z \hat{I}_+ + \hat{I}_+ \hat{I}_z) \hat{\sigma}_- + (\hat{I}_z \hat{I}_- + \hat{I}_- \hat{I}_z) \hat{\sigma}_+ \right] + Q_2^{(e)} \left[\hat{I}_-^2 \hat{\sigma}_- + \hat{I}_+^2 \hat{\sigma}_+ \right] + \\ &A_1^{(e)} \left[(\hat{I}_z \hat{S}_+ + \hat{I}_+ \hat{S}_z) \hat{\sigma}_- + (\hat{I}_z \hat{S}_- + \hat{I}_- \hat{S}_z) \hat{\sigma}_+ \right] + A_2^{(e)} \left[(\hat{S}_- \hat{I}_- \hat{\sigma}_- + \hat{S}_+ \hat{I}_+ \hat{\sigma}_+ \right], \end{aligned} \quad (4)$$

where $D_{1,2}^{(e)}$, $Q_{1,2}^{(e)}$ and $A_{1,2}^{(e)}$ are the respective tensor el-

more complicated with possessing quadrupole moment (Q) than the ^{13}C $I = 1/2$ nuclear spin. The spin Hamiltonian of the ground state reads as

$$\begin{aligned} \hat{H}_0 &= D \left(\hat{S}_z^2 - \frac{1}{3} S(S+1) \right) + Q \left(\hat{I}_z^2 - \frac{1}{3} I(I+1) \right) + \\ &A_{\parallel} \hat{S}_z \hat{I}_z + \frac{1}{2} A_{\perp} \left(\hat{S}_+ \hat{I}_- + \hat{S}_- \hat{I}_+ \right), \end{aligned} \quad (2)$$

where S_z and I_z are the respective electron and nuclear spin quantum numbers, A_{\parallel} and A_{\perp} are the respective components of the electron spin-nuclear spin hyperfine tensor which is parallel diagonal with the zero-field splitting tensor as the N ion sits in the C_{3v} axis which does not generally hold for the ^{13}C ions. The spin shift \hat{S}_{\pm} and \hat{I}_{\pm} operators can be generally defined as $\hat{\Gamma}_{\pm} = (\hat{\Gamma}_x \pm i \hat{\Gamma}_y) / \sqrt{2}$.

In the ground (g) state, $D^{(g)} = 2.87$ GHz, $Q^{(g)} = -4.96$ MHz, $A_{\parallel}^{(g)} = -2.16$ MHz, and $A_{\perp}^{(g)} = -2.70$ MHz [49] which is weakly susceptible to strain [50]. On the other hand, ^{14}N spins exhibit long coherence and relaxation times [51, 52] similarly to that of ^{13}C nuclear spins [53, 54] that makes ^{14}N nuclear spin readout possible even at room temperature [55]. As $D \gg A_{\perp}$ the nuclear spin-flip is much suppressed unless the external magnetic field is used to compensate the D gap between the $m_S = 0$ and $m_S = -1$ or $m_S = +1$ levels (so called ground state level anticrossing regime [56, 57]). We discuss further the zero or low magnetic field regime where such nuclear spin-flip does not occur.

We turn to the analysis of the optical $|^3E\rangle$ excited state. The static C_{3v} Hamiltonian for $|^3E\rangle$ reads as the sum of Eq. 2 and

$$\begin{aligned} \hat{H}_{\text{SO}} &= \lambda^{(e)} \hat{\sigma}_z \hat{S}_z = \lambda^{(e)} \left(|A_1\rangle \langle A_1| + |A_2\rangle \langle A_2| \right. \\ &\quad \left. - |E_1\rangle \langle E_1| - |E_2\rangle \langle E_2| \right), \end{aligned} \quad (3)$$

where \hat{H}_{SO} enters because of the orbital degeneracy of the excited state where $\hat{\sigma}_z = |e_+\rangle \langle e_+| - |e_-\rangle \langle e_-|$ operator describes the orbital moment. For the same reason, JT effect appears which dynamically breaks the C_{3v} symmetry which is manifested in the zero-field splitting, quadrupole and hyperfine tensors. After introducing the $\hat{\sigma}_{\pm} = |e_{\mp}\rangle \langle e_{\pm}|$ orbital flipping operators the spin-phonon interaction may be expressed as

elements. $D_1^{(e)}$ mixes $|E_{1,2}\rangle$ with $|E_{x,y}\rangle$, and $D_2^{(e)}$ splits

$|A_1\rangle$ and $|A_2\rangle$ levels. Additionally to the A_{\perp} hyperfine parameter, $A_{1,2}^{(e)}$ and $Q_{1,2}^{(e)}$ dynamical interactions may also flip the nuclear spin. Parameters $D^{(e)} = 1.42$ GHz, $\lambda^{(e)} = 5.3$ GHz and $2 \times D_2^{(e)} = 1.55$ GHz are directly observed in the photoluminescence excitation spectroscopy whereas $\sqrt{2}D_1^{(e)} = 200$ MHz was approximately deduced from the observed rates (see references in Ref. 45). $A_{\parallel}^{(e)} \approx 40$ MHz and $A_{\perp}^{(e)} \approx 27$ MHz for ^{14}N were observed already [58, 59] whereas $A_{1,2}^{(e)}$ and $Q^{(e)}$, $Q_1^{(e)}$ and $Q_2^{(e)}$ parameters have been not yet observed to our knowledge. In order to obtain these critical parameters, we develop and implement an *ab initio* theory.

The dynamical nature of the wavefunction may be written as $|e_{\varphi}\rangle = \cos(\varphi/2)|e_x\rangle + \sin(\varphi/2)|e_y\rangle$, where φ is a rotation angle defined by X and Y configurational coordinates of the APES as depicted in Fig. 2.

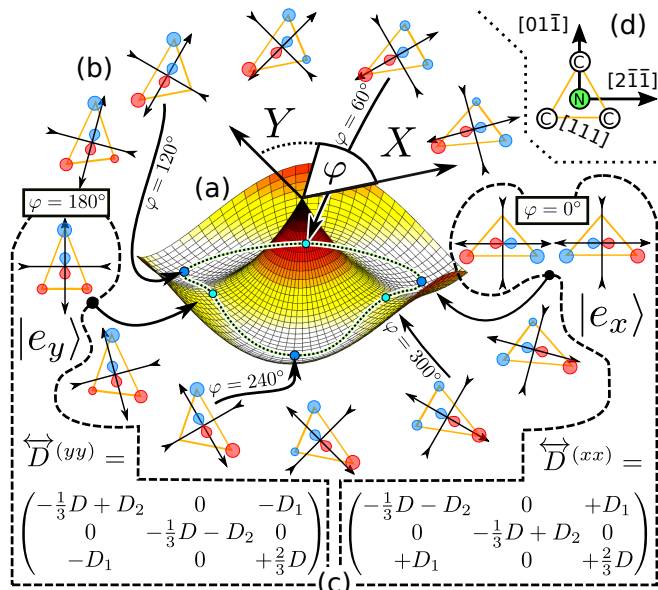


FIG. 2. Dynamic Jahn-Teller effect in $|^3E\rangle$ for NV center. (a) Adiabatic potential energy surface (APES) for NV center in diamond as calculated in Ref. 43. (b) Transformation of the occupied $|e_{\varphi}\rangle = \cos(\frac{\varphi}{2})|e_x\rangle - \sin(\frac{\varphi}{2})|e_y\rangle$ orbital where we omit the $e^{\pm i\varphi\pi/360^\circ}$ phase factor that would remove the discontinuity at $\varphi = 0$. We show the wavefunctions on three carbon vacancy lobes plus the “ $2p$ ” character on the central N atom. (d) Zero-field splitting tensors $\overleftrightarrow{D}^{(xx)}$ and $\overleftrightarrow{D}^{(yy)}$ at $\varphi = 0^\circ$ and 180° pseudorotations [60–64], respectively. The $^{(xx)}$, $^{(yy)}$ superscripts refer to whenever $|e_x\rangle$ or $|e_y\rangle$ orbital is occupied. (c) Geometry of the undistorted system. We depict the [111] oriented coordinate system used for $\overleftrightarrow{D}^{(\dots)}$ tensors.

We are interested in the values of second rank tensors ($\overleftrightarrow{\Gamma} = \{\overleftrightarrow{D}, \overleftrightarrow{A}, \overleftrightarrow{Q}\}$) describing spin-spin interactions. We control whether $|e_x\rangle$ or $|e_y\rangle$ orbital is being occupied by relaxing the atomic positions to reach the JT distorted minimum or to the saddle point between the JT minima. Therefore, one may yield different $\overleftrightarrow{\Gamma}^{(xx)}$ or $\overleftrightarrow{\Gamma}^{(yy)}$ ten-

TABLE I. Theoretical and (experimental) spin parameters for NV center in diamond

$\lambda_1^{(e)} =$	4.8 ^a (5.3 ^b)	$D^{(g)} =$	2.98 (2.87 ^e) GHz
$A_{\parallel}^{(g)} =$	-1.7 ^c (-2.14 ^d) MHz	$D^{(e)} =$	1.67 (1.42 ^e) GHz
$A_{\perp}^{(g)} =$	-1.7 ^c (-2.70 ^d) MHz	$D_1^{(e)} =$	-290 (200/ $\sqrt{2}$ ^e) MHz
$A_{\parallel}^{(e)} =$	-41 (-40 ^f) MHz	$D_2^{(e)} =$	+901 (1550/2 ^e) MHz
$A_{\perp}^{(e)} =$	-27 (-23 ^g) MHz	$\overline{Q}^{(g)} =$	-5.37 ^h (-4.95 ^h) MHz
$A_1^{(e)} =$	-92 (n.a.) kHz	$Q^{(e)} =$	-3.91 (n.a.) MHz
$A_2^{(e)} =$	+49 (n.a.) kHz	$Q_1^{(e)} =$	+17.3 (n.a.) kHz
$\tau_{\text{rad}}^{-1} =$	n.a. (83 ⁱ) MHz	$Q_2^{(e)} =$	+17.2 (n.a.) kHz

^a *Ab initio* result [43] by means of HSE06 [30] functional

^b Expt. data vary between 5.3 GHz [65] and 5.33(3) GHz [66]

^c *Ab initio* result [49] by means of LDA [67] (local density approximation)

^d Measured via electron paramagnetic resonance [68]. Similar values were measured in Refs. 69 and 70 for example.

^e Experimental values are taken from Refs. 45 or 65

^f Measured via ESLAC, see Ref. 59

^g Measured via ESLAC, see Ref. 58

^h *Ab initio* result [71] by means of HSE06 [30] functional.

Experimental result is also taken from Ref. 71. Similar values were measured in Refs. 68–70 for example.

ⁱ See Refs. 72–75 for radiative lifetime of $|^3E\rangle$

sors whether $|e_x\rangle$ or $|e_y\rangle$ orbitals are being occupied. We note that, in principle, one may obtain $\overleftrightarrow{\Gamma}(\varphi)$ at any desired φ angle. However, we take $\overleftrightarrow{\Gamma}^{(xx)}$ tensors evaluated at the JT minimum ($\varphi = 0^\circ$) for the sake of simplicity.

After group theory derivation [76] one may find that the diagonal terms appearing in Eq. (2) can be formulated as $\Gamma = \Gamma_{zz}^{(xx)} - (\Gamma_{xx}^{(xx)} + \Gamma_{yy}^{(xx)})/2$ for D and Q parameters. We note that the trace of \overleftrightarrow{A} is not zero, in contrast to \overleftrightarrow{D} and \overleftrightarrow{Q} , thus hyperfine interaction comes with two independent parameters $A_{\parallel} = A_{zz}^{(xx)}$ and $A_{\perp} = (A_{xx}^{(xx)} + A_{yy}^{(xx)})/2$.

The orbital flipping terms in Eq. (4) can be interpreted as dynamic deviations of $\overleftrightarrow{\Gamma}$ tensors from C_{3v} symmetry. That is, the presence of an $|e_x\rangle$ orbital spontaneously breaks the trigonal symmetry thus additional terms appear violating the C_{3v} symmetry. One may use these terms to determine $\Gamma_1 = \Gamma_{xz}^{(xx)}$ and $\Gamma_2 = D_{xy}^{(xx)}$, respectively.

However, Γ_1 and Γ_2 are subject of the so-called Ham reduction [77] due to the strong electron-phonon coupling by partially averaging out the orbital degrees of freedom during the dynamic JT motion. In our particular case, we deal with $E \otimes e$ JT system for which Bersuker gave a recipe to estimate the Ham reduction factors p and q (see Refs. 63 and 64 for details). We already showed that the spin-orbit λ is reduced by $p = 0.304$ as $\hat{\sigma}_z$ transforms as A_2 under C_{3v} symmetry [43]. The Γ_1 and Γ_2 interactions transform as E and thus their values are reduced by q factor. There is a connection between p and q that results in $q = (1+p)/2 = 0.652$ that is practically valid for multi

JT approach [78]. Finally, we note that the frequency of JT tunneling is orders of magnitude faster than that of all spin interactions that are discussed here, thus one may use the p , q reduction factors as the vibronically entangled JT states remain dressed.

The final calculated values are $Q_1^{(e)} \approx 17.3$ kHz, $Q_2^{(e)} \approx 17.2$ kHz, $A_1^{(e)} \approx 92.2$ kHz, and $A_2^{(e)} \approx 48.9$ kHz. Furthermore, $Q^{(e)} = -3.91$ MHz is obtained. We note that the calculated values for $D^{(e)} = 1.67$ GHz, $D_1^{(e)} \approx -289$ MHz and $D_2^{(e)} \approx 901$ MHz as well as the $A_{\parallel}^{(e)} = -41$ MHz, $A_{\perp}^{(e)} = -27$ MHz agree with the known experimental data (see Table I for comparison; the sign of the values cannot be determined in the experiments). Thus, we have all the parameters in our hand to compute the nuclear spin relaxation rates.

We assume that the NV center is first initialized into the $m_S = 0$ of the $|^3A_2\rangle$ ground state and then upon illumination it is excited to $|E_x\rangle$ or $|E_y\rangle$ which are often split in real experiments because of the presence of strain. The electron stays about $\tau_{\text{rad}} \approx 12$ ns in this excited before it decays to the ground state [72–75]. During this time interval we examine which terms of the full Hamiltonian $\hat{H} = \hat{H}_0 + \hat{H}_{\text{SO}} + \hat{W}$ (sum of Eqs. (2), (3), (4)) may rotate the nuclear spin. Therefore, we examine the terms that contain nuclear spin-flip operators. These terms are $A_{\perp}^{(e)}$, $A_1^{(e)}$, $A_2^{(e)}$ hyperfine and $Q_1^{(e)}$, $Q_2^{(e)}$ quadrupolar parameters (Fig. 3).

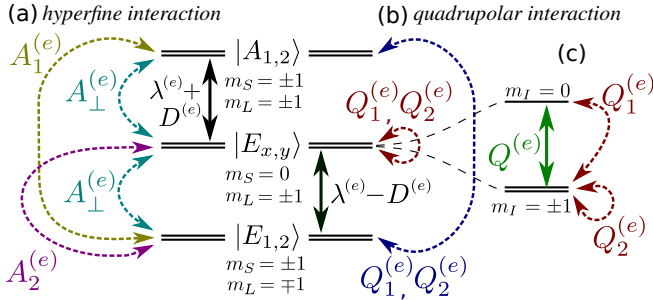


FIG. 3. Interactions involving nuclear spin-flip processes. We show the terms appearing due to nuclear quadrupolar and hyperfine interactions in (a) and (b), respectively. For the sake of simplicity, we neglect the effect of D_1 and D_2 . (c) $|E_{x,y}\rangle \otimes |m_I\rangle$ states are split further by means of quadrupolar $Q^{(e)}$ parameter.

We pick up $|E_x\rangle$ with $|0\rangle$ nuclear spin state then the perpendicular component of the hyperfine interaction mixes in the state as

$$\begin{aligned} |E_x\rangle \otimes |0\rangle &= |E_x\rangle \otimes |0\rangle + \\ \frac{A_{\perp}^{(e)}}{\lambda^{(e)} - D^{(e)}} \times \frac{|E_1\rangle \otimes |x\rangle - |E_2\rangle \otimes |y\rangle}{\sqrt{2}} \end{aligned} \quad (5)$$

within first order of perturbation, where we used real valued basis for ^{14}N spins for simplicity: $|\pm 1\rangle = (|x\rangle \pm$

$i|y\rangle)/\sqrt{2}$. We note that the Fermi's golden rule is valid because the Rabi-oscillation between the spin states is three orders of magnitude faster than the inverse lifetime of the electronic excited state. Therefore, according to Fermi's golden rule there is a $(A_{\perp}^{(e)}/(\lambda^{(e)} - D^{(e)}))^2 = 3.5 \times 10^{-5}$ probability for ^{14}N spin to relax from $|0\rangle$ to any of $|\pm\rangle$ at each optical cycle. We note that $A_1^{(e)}$, $A_2^{(e)}$ terms are negligibly small compared to $A_{\perp}^{(e)}$, thus we omit them from further discussion.

Next, we discuss the $Q_1^{(e)}$, $Q_2^{(e)}$ quadrupolar parameters. The effect of $Q_2^{(e)}$ within Eq. (4) would be

$$\begin{aligned} Q_2^{(e)} [\hat{I}_-^2 \hat{\sigma}_- + \hat{I}_+^2 \hat{\sigma}_+] |E_{\mp}\rangle \otimes |\pm\rangle &= 2Q_2 |E_{\pm}\rangle \otimes |\mp\rangle \\ Q_2^{(e)} [\hat{I}_-^2 \hat{\sigma}_- + \hat{I}_+^2 \hat{\sigma}_+] |E_{\pm}\rangle \otimes |\pm\rangle &= 0, \end{aligned} \quad (6)$$

which resembles the effect of excited state level state anticrossing [56, 79–81] (ESLAC) but without any applied magnetic field. Therefore, the perturbative approach that of Eqs. (5) is not valid here. The solution will be the following entangled eigenstates,

$$\Psi_{\pm} = \frac{1}{\sqrt{2}} |E_{+}\rangle \otimes |-\rangle \pm \frac{1}{\sqrt{2}} |E_{-}\rangle \otimes |+\rangle, \quad (7)$$

separated by $4Q_2$ energy from each other. This offers very efficient $\Delta m_I = \pm 2$ flipping channel. However, Fermi's golden rule is violated this time since $\tau_{\text{rad}}^{-1} \not\ll Q_2^{(e)}$. In simple words, $\tau_{\text{rad}} = 12$ ns is simply not sufficient for time averaging the $\langle \sin^2(Q_2^{(e)} t) \rangle = \frac{1}{2}$ Rabi oscillation with $1/Q_2^{(e)} = 58 \mu\text{s}$ period time between $|E_{+}\rangle \otimes |-\rangle \leftrightarrow |E_{-}\rangle \otimes |+\rangle$ states. Therefore, we propagate the Schrödinger equation appropriately and thus arrive at negligibly small $\int_0^{\infty} \frac{1}{\tau_{\text{rad}}} e^{-t/\tau_{\text{rad}}} (2Q_2)^2 t^2 dt = 4Q_2^2 \tau_{\text{rad}}^2 = 1.7 \times 10^{-7}$ probability.

However, in typical optical qubit preparation and readout protocols excitation into the $|^3E\rangle$ manifold is consecutively repeated many times where the readout time usually varies around the microsecond regime [55, 81–84]. For example, $20 \mu\text{s}$ readout time were utilized in Ref. 84 while exciting the $m_S = 0$ transition. The excitation of NV center is saturated, so the system stays minimal duration within the $|^3A_2\rangle$ ground state. Therefore, there are $n = 20 \mu\text{s}/12 \text{ ns} = 1667$ cycles that leads to $1667 \times 4.8 \times 10^{-5} = 8\%$ ^{14}N spin flipping probability mediated by $A_{\perp}^{(e)}$ interaction. We note that our result agrees with the experimental observation that ^{15}N nuclear spin acting as quantum memory supports only $n \approx 1000$ consecutive optical readouts before destruction [25].

On the other hand, the Rabi oscillation time for Q_2 adds up coherently that effectively elongates the evolution within the excited state, thus the transition probability will be $\sim 11\%$ as shown in Table II see Ref. 76 for details where we also included the effect of local strain splitting of $|E_x\rangle$ and $|E_y\rangle$. This approximation is true as long as the full readout or preparation time is within

TABLE II. Theoretical and experimental ^{14}N spin-flip probabilities for 20 μs readout time. See Table 2 in Supp. Mat. that of Ref. 84 for experimental data on which we summed the $m_S = \pm 1$ spin degrees of freedom for clarity. For actual derivation of theoretical results we refer to Ref. 76.

transition	theory	expt.
$ m_I = \pm 1\rangle \rightarrow m_I = \mp 1\rangle$	0.11	0.18(3)
$ m_I = \pm 1\rangle \rightarrow m_I = 0\rangle$	0.08	0.16(3)
$ m_I = 0\rangle \rightarrow m_I = \pm 1\rangle$	0.16	0.25(3)

the coherence time of the nuclear spin. Therefore, if the readout is longer than the coherence time, one may suppress $\Delta m_I = \pm 2$ flips. Finally, we note that the effect of Q_1 magnitudes smaller than that of $A_{\perp}^{(e)}$ and $Q_2^{(e)}$ since it is suppressed by the $Q^{(e)}$ quadrupolar parameter that we depict in Fig. 3 while $Q_2^{(e)}$ may rotate the ^{14}N spin freely.

In summary, (i) we computed D , A , Q tensors including the non-trivial terms mediated by electron-phonon coupling at *ab initio* level that appear due to orbital degeneracy of $|^3E\rangle$. Secondly, (ii) our results point to non-negligible $\Delta m_I = \pm 2$ nuclear spin-flip channels during repeated optical cycles towards $|^3E\rangle$ mediated by $Q_2^{(e)}(\hat{I}_-^2\hat{\sigma}_- + \hat{I}_+^2\hat{\sigma}_+)$ quadrupolar terms while $\frac{1}{2}A_{\perp}(\hat{S}_+\hat{I}_- + \hat{S}_-\hat{I}_+)$ hyperfine interaction is responsible for $\Delta m_I = \pm 1$ transitions. (iii) From experimental point of view, our findings indicate that long optical readout or preparation times in the μs regime may hinder the fidelity of qubit applications utilizing ^{14}N nuclear spin. The upper $|^3E\rangle$ triplet endures additional spin-flip channels not present at the $|^3A_2\rangle$ ground state, thus our results suggest that optical ^{14}N nuclear spin read out protocols for NV should not exceed a few microseconds. These findings are relevant to other solid state qubits. NV centers in silicon carbide (SiC) [85, 86] trivially belong to this category; spin flipping terms for half spin nuclear spins do apply for divacancy qubits in SiC [87–89] and can be potentially applied to other defect qubits (e.g., Ref. 90) that exhibit strong electron-phonon coupling in their electronic excited state.

Support by the National Excellence Program of the National Research, Development and Innovation Office (NKFIH) as well as by the Ministry of Culture and Innovation within the Quantum Information National Laboratory of Hungary (Grant No. 2022-2.1.1-NL-2022-00004) is much appreciated. AG acknowledges the high-performance computational resources provided by KIFÜ (Governmental Agency for IT Development) institute of Hungary, the European Commission for the projects QuMicro (Grant No. 101046911) and SPINUS (Grant No. 101135699) and the QuantERA II project Maestro.

- [1] J. Weber, W. Koehl, J. Varley, A. Janotti, B. Buckley, C. Van de Walle, and D. D. Awschalom, *Proceedings of the National Academy of Sciences* **107**, 8513 (2010).
- [2] J. Wrachtrup and F. Jelezko, *Journal of Physics: Condensed Matter* **18**, S807–S824 (2006).
- [3] S. Praver and I. Aharonovich, *Quantum information processing with diamond: principles and applications* (Elsevier, 2014).
- [4] J. Zhang, S. S. Hegde, and D. Suter, *Phys. Rev. Lett.* **125**, 030501 (2020).
- [5] Z.-H. Zhang, P. Stevenson, G. Thiering, B. C. Rose, D. Huang, A. M. Edmonds, M. L. Markham, S. A. Lyon, A. Gali, and N. P. de Leon, *Physical Review Letters* **125**, 237402 (2020).
- [6] G. Wolfowicz, F. J. Heremans, C. P. Anderson, S. Kanai, H. Seo, A. Gali, G. Galli, and D. D. Awschalom, *Nature Reviews Materials* **6**, 906 (2021).
- [7] M. W. Doherty, N. B. Manson, P. Delaney, F. Jelezko, J. Wrachtrup, and L. C. Hollenberg, *Physics Reports* **528**, 1–45 (2013).
- [8] A. Gali, *Nanophotonics* **8**, 1907–1943 (2019).
- [9] L. Childress, M. V. Gurudev Dutt, J. M. Taylor, A. S. Zibrov, F. Jelezko, J. Wrachtrup, P. R. Hemmer, and M. D. Lukin, *Science* **314**, 281–285 (2006).
- [10] T. van der Sar, Z. H. Wang, M. S. Blok, H. Bernien, T. H. Taminiau, D. M. Toyli, D. A. Lidar, D. D. Awschalom, R. Hanson, and V. V. Dobrovitski, *Nature* **484**, 82–86 (2012).
- [11] D. A. Golter, K. N. Dinyari, and H. Wang, *Phys. Rev. A* **87**, 035801 (2013).
- [12] T. H. Taminiau, J. Cramer, T. van der Sar, V. V. Dobrovitski, and R. Hanson, *Nature Nanotechnology* **9**, 171–176 (2014).
- [13] G. Waldherr, Y. Wang, S. Zaiser, M. Jamali, T. Schulte-Herbrüggen, H. Abe, T. Ohshima, J. Isoya, J. F. Du, P. Neumann, and J. Wrachtrup, *Nature* **506**, 204–207 (2014).
- [14] I. Lovchinsky, A. O. Sushkov, E. Urbach, N. P. de Leon, S. Choi, K. De Greve, R. Evans, R. Gertner, E. Bersin, C. Müller, L. McGuinness, F. Jelezko, R. L. Walsworth, H. Park, and M. D. Lukin, *Science* **351**, 836–841 (2016).
- [15] A. Reiserer, N. Kalb, M. S. Blok, K. J. M. van Bemmelen, T. H. Taminiau, R. Hanson, D. J. Twitchen, and M. Markham, *Phys. Rev. X* **6**, 021040 (2016).
- [16] M. H. Abobeih, J. Cramer, M. A. Bakker, N. Kalb, M. Markham, D. J. Twitchen, and T. H. Taminiau, *Nature Communications* **9** (2018), 10.1038/s41467-018-04916-z.
- [17] G. Murta, S. B. van Dam, J. Ribeiro, R. Hanson, and S. Wehner, *Quantum Science and Technology* **4**, 035011 (2019).
- [18] C. E. Bradley, J. Randall, M. H. Abobeih, R. C. Berrevoets, M. J. Degen, M. A. Bakker, M. Markham, D. J. Twitchen, and T. H. Taminiau, *Phys. Rev. X* **9**, 031045 (2019).
- [19] M. Ruf, N. H. Wan, H. Choi, D. Englund, and R. Hanson, *Journal of Applied Physics* **130** (2021), 10.1063/5.0056534.
- [20] G. L. van de Stolpe, D. P. Kwiatkowski, C. E. Bradley, J. Randall, S. A. Breitweiser, L. C. Bassett, M. Markham, D. J. Twitchen, and T. H. Taminiau, “Mapping a 50-

- spin-qubit network through correlated sensing,” (2023), [arXiv:2307.06939](https://arxiv.org/abs/2307.06939) [quant-ph].
- [21] M. V. G. Dutt, L. Childress, L. Jiang, E. Togan, J. Maze, F. Jelezko, A. S. Zibrov, P. R. Hemmer, and M. D. Lukin, *Science* **316**, 1312–1316 (2007).
- [22] G. D. Fuchs, V. V. Dobrovitski, D. M. Toyli, F. J. Heremans, C. D. Weis, T. Schenkel, and D. D. Awschalom, *Nature Physics* **6**, 668–672 (2010).
- [23] G. D. Fuchs, G. Burkard, P. V. Klimov, and D. D. Awschalom, *Nature Physics* **7**, 789–793 (2011).
- [24] J. Casanova, Z.-Y. Wang, and M. B. Plenio, *Phys. Rev. Lett.* **117**, 130502 (2016).
- [25] T. Roskopf, J. Zopes, J. M. Boss, and C. L. Degen, *npj Quantum Information* **3** (2017), [10.1038/s41534-017-0030-6](https://doi.org/10.1038/s41534-017-0030-6).
- [26] G.-Q. Liu, J. Xing, W.-L. Ma, P. Wang, C.-H. Li, H. C. Po, Y.-R. Zhang, H. Fan, R.-B. Liu, and X.-Y. Pan, *Phys. Rev. Lett.* **118**, 150504 (2017).
- [27] V. V. Soshenko, S. V. Bolshedvorskii, O. Rubinas, V. N. Sorokin, A. N. Smolyaninov, V. V. Vorobyov, and A. V. Akimov, *Phys. Rev. Lett.* **126**, 197702 (2021).
- [28] J.-P. Tetienne, L. T. Hall, A. J. Healey, G. A. L. White, M.-A. Sani, F. Separovic, and L. C. L. Hollenberg, *Phys. Rev. B* **103**, 014434 (2021).
- [29] A. Dréau, P. Spinicelli, J. R. Maze, J.-F. Roch, and V. Jacques, *Phys. Rev. Lett.* **110**, 060502 (2013).
- [30] J. Heyd, G. E. Scuseria, and M. Ernzerhof, *The Journal of Chemical Physics* **118**, 8207 (2003).
- [31] P. E. Blöchl, *Phys. Rev. B* **62**, 6158 (2000).
- [32] O. V. Yazyev, I. Tavernelli, L. Helm, and U. Röthlisberger, *Phys. Rev. B* **71**, 115110 (2005).
- [33] K. Szász, T. Hornos, M. Marsman, and A. Gali, *Phys. Rev. B* **88**, 075202 (2013).
- [34] Z. Bodrog and A. Gali, *Journal of Physics: Condensed Matter* **26**, 015305 (2013).
- [35] H. M. Petrilli, P. E. Blöchl, P. Blaha, and K. Schwarz, *Phys. Rev. B* **57**, 14690 (1998).
- [36] A. Gali, E. Janzén, P. Deák, G. Kresse, and E. Kaxiras, *Physical Review Letters* **103**, 186404 (2009).
- [37] J. P. Perdew, K. Burke, and M. Ernzerhof, *Physical Review Letters* **77**, 3865 (1996).
- [38] G. Kresse and J. Hafner, *Phys. Rev. B* **49**, 14251 (1994).
- [39] G. Kresse and J. Furthmüller, *Physical Review B* **54**, 11169 (1996).
- [40] G. Kresse and J. Furthmüller, *Computational Materials Science* **6**, 15–50 (1996).
- [41] K.-M. C. Fu, C. Santori, P. E. Barclay, L. J. Rogers, N. B. Manson, and R. G. Beausoleil, *Physical Review Letters* **103**, 256404 (2009).
- [42] T. A. Abtew, Y. Y. Sun, B.-C. Shih, P. Dev, S. B. Zhang, and P. Zhang, *Physical Review Letters* **107**, 146403 (2011).
- [43] G. Thiering and A. Gali, *Physical Review B* **96**, 081115 (2017).
- [44] P. E. Blöchl, *Physical Review B* **50**, 17953 (1994).
- [45] M. W. Doherty, N. B. Manson, P. Delaney, and L. C. L. Hollenberg, *New Journal of Physics* **13**, 025019 (2011).
- [46] J. R. Maze, A. Gali, E. Togan, Y. Chu, A. Trifonov, E. Kaxiras, and M. D. Lukin, *New Journal of Physics* **13**, 025025 (2011).
- [47] R. Ulbricht, S. Dong, I.-Y. Chang, B. M. K. Mariserla, K. M. Dani, K. Hyeon-Deuk, and Z.-H. Loh, *Nature Communications* **7** (2016), [10.1038/ncomms13510](https://doi.org/10.1038/ncomms13510).
- [48] R. Ulbricht, S. Dong, A. Gali, S. Meng, and Z.-H. Loh, *Phys. Rev. B* **97**, 220302 (2018).
- [49] A. Gali, M. Fyta, and E. Kaxiras, *Phys. Rev. B* **77**, 155206 (2008).
- [50] P. Udvarhelyi, V. O. Shkolnikov, A. Gali, G. Burkard, and A. Pályi, *Phys. Rev. B* **98**, 075201 (2018).
- [51] L. Busaite, R. Lazda, A. Berzins, M. Auzinsh, R. Ferber, and F. Gahbauer, *Phys. Rev. B* **102**, 224101 (2020).
- [52] H. Morishita, S. Kobayashi, M. Fujiwara, H. Kato, T. Makino, S. Yamasaki, and N. Mizuochi, *Scientific Reports* **10** (2020), [10.1038/s41598-020-57569-8](https://doi.org/10.1038/s41598-020-57569-8).
- [53] B. Scharfenberger, W. J. Munro, and K. Nemoto, *New Journal of Physics* **16**, 093043 (2014).
- [54] P. C. Maurer, G. Kucsko, C. Latta, L. Jiang, N. Y. Yao, S. D. Bennett, F. Pastawski, D. Hunger, N. Chisholm, M. Markham, D. J. Twitchen, J. I. Cirac, and M. D. Lukin, *Science* **336**, 1283–1286 (2012).
- [55] M. Gulka, D. Wirtitsch, V. Ivády, J. Vodnik, J. Hruby, G. Magchiels, E. Bourgeois, A. Gali, M. Trupke, and M. Nesladek, *Nature Communications* **12** (2021), [10.1038/s41467-021-24494-x](https://doi.org/10.1038/s41467-021-24494-x).
- [56] V. Jacques, P. Neumann, J. Beck, M. Markham, D. Twitchen, J. Meijer, F. Kaiser, G. Balasubramanian, F. Jelezko, and J. Wrachtrup, *Phys. Rev. Lett.* **102**, 057403 (2009).
- [57] A. Gali, *Phys. Rev. B* **79**, 235210 (2009).
- [58] F. Poggiali, P. Cappellaro, and N. Fabbri, *Phys. Rev. B* **95**, 195308 (2017).
- [59] M. Steiner, P. Neumann, J. Beck, F. Jelezko, and J. Wrachtrup, *Phys. Rev. B* **81**, 035205 (2010).
- [60] T. C. Thompson, D. G. Truhlar, and C. A. Mead, *The Journal of Chemical Physics* **82**, 2392–2407 (1985).
- [61] F. Cocchini, T. H. Upton, and W. Andreoni, *The Journal of Chemical Physics* **88**, 6068–6077 (1988).
- [62] I. B. Bersuker, *Chemical Reviews* **101**, 1067–1114 (2001).
- [63] I. Bersuker, *The Jahn-Teller effect* (Cambridge University Press, 2006).
- [64] I. Bersuker and V. Polinger, *Vibronic interactions in molecules and crystals*, Vol. 49 (Springer Science & Business Media, 2012).
- [65] A. Batalov, V. Jacques, F. Kaiser, P. Siyushev, P. Neumann, L. J. Rogers, R. L. McMurtrie, N. B. Manson, F. Jelezko, and J. Wrachtrup, *Phys. Rev. Lett.* **102**, 195506 (2009).
- [66] L. C. Bassett, F. J. Heremans, D. J. Christle, C. G. Yale, G. Burkard, B. B. Buckley, and D. D. Awschalom, *Science* **345**, 1333–1337 (2014).
- [67] J. P. Perdew and S. Kurth, “Density functionals for non-relativistic coulomb systems in the new century,” in *A Primer in Density Functional Theory* (Springer Berlin Heidelberg, 2003) p. 1–55.
- [68] S. Felton, A. M. Edmonds, M. E. Newton, P. M. Martineau, D. Fisher, D. J. Twitchen, and J. M. Baker, *Phys. Rev. B* **79**, 075203 (2009).
- [69] B. Rose, C. Weis, A. Tyryshkin, T. Schenkel, and S. Lyon, *Diamond and Related Materials* **72**, 32–40 (2017).
- [70] X.-F. He, N. B. Manson, and P. T. H. Fisk, *Phys. Rev. B* **47**, 8816 (1993).
- [71] M. Pfender, N. Aslam, P. Simon, D. Antonov, G. Thiering, S. Burk, F. Fávoro de Oliveira, A. Denisenko, H. Fedder, J. Meijer, J. A. Garrido, A. Gali, T. Teraji, J. Isoya, M. W. Doherty, A. Alkauskas, A. Gallo, A. Grüneis, P. Neumann, and J. Wrachtrup, *Nano Letters* **17**, 5931–5937 (2017).

- [72] L. Robledo, H. Bernien, T. v. d. Sar, and R. Hanson, *New Journal of Physics* **13**, 025013 (2011).
- [73] D. M. Toyli, D. J. Christle, A. Alkauskas, B. B. Buckley, C. G. Van de Walle, and D. D. Awschalom, *Phys. Rev. X* **2**, 031001 (2012).
- [74] M. L. Goldman, M. W. Doherty, A. Sipahigil, N. Y. Yao, S. D. Bennett, N. B. Manson, A. Kubanek, and M. D. Lukin, *Phys. Rev. B* **91**, 165201 (2015).
- [75] M. L. Goldman, A. Sipahigil, M. W. Doherty, N. Y. Yao, S. D. Bennett, M. Markham, D. J. Twitchen, N. B. Manson, A. Kubanek, and M. D. Lukin, *Phys. Rev. Lett.* **114**, 145502 (2015).
- [76] “See supplemental material.”
- [77] F. S. Ham, *Phys. Rev.* **138**, A1727 (1965).
- [78] S. N. Evangelou, M. C. M. O’Brien, and R. S. Perkins, *Journal of Physics C: Solid State Physics* **13**, 4175–4198 (1980).
- [79] R. Fischer, A. Jarmola, P. Kehayias, and D. Budker, *Phys. Rev. B* **87**, 125207 (2013).
- [80] V. Ivády, K. Szász, A. L. Falk, P. V. Klimov, D. J. Christle, E. Jánzén, I. A. Abrikosov, D. D. Awschalom, and A. Gali, *Phys. Rev. B* **92**, 115206 (2015).
- [81] A. Jarmola, I. Fescenko, V. M. Acosta, M. W. Doherty, F. K. Fatemi, T. Ivanov, D. Budker, and V. S. Malinovsky, *Physical Review Research* **2** (2020), 10.1103/physrevresearch.2.023094.
- [82] D. Hopper, H. Shulevitz, and L. Bassett, *Micromachines* **9**, 437 (2018).
- [83] D. M. Irber, F. Poggiali, F. Kong, M. Kieschnick, T. Lühmann, D. Kwiatkowski, J. Meijer, J. Du, F. Shi, and F. Reinhard, *Nature Communications* **12** (2021), 10.1038/s41467-020-20755-3.
- [84] R. Monge, T. Delord, G. Thiering, A. Gali, and C. A. Meriles, *Phys. Rev. Lett.* **131**, 236901 (2023).
- [85] Z. Mu, S. A. Zargaleh, H. J. von Bardeleben, J. E. Fr’och, M. Nonahal, H. Cai, X. Yang, J. Yang, X. Li, I. Aharonovich, and W. Gao, *Nano Letters* **20**, 6142 (2020), pMID: 32644809, <https://doi.org/10.1021/acs.nanolett.0c02342>.
- [86] J.-F. Wang, F.-F. Yan, Q. Li, Z.-H. Liu, H. Liu, G.-P. Guo, L.-P. Guo, X. Zhou, J.-M. Cui, J. Wang, Z.-Q. Zhou, X.-Y. Xu, J.-S. Xu, C.-F. Li, and G.-C. Guo, *Phys. Rev. Lett.* **124**, 223601 (2020).
- [87] W. F. Koehl, B. B. Buckley, F. J. Heremans, G. Calusine, and D. D. Awschalom, *Nature* **479**, 84 (2011).
- [88] D. J. Christle, A. L. Falk, P. Andrich, P. V. Klimov, J. U. Hassan, N. T. Son, E. Jánzén, T. Ohshima, and D. D. Awschalom, *Nature Materials* **14**, 160 (2015).
- [89] D. J. Christle, P. V. Klimov, C. F. de las Casas, K. Szász, V. Ivády, V. Jokubavicius, J. Ul Hassan, M. Syväjärvi, W. F. Koehl, T. Ohshima, N. T. Son, E. Jánzén, A. Gali, and D. D. Awschalom, *Phys. Rev. X* **7**, 021046 (2017).
- [90] G. Zhang, Y. Cheng, J.-P. Chou, and A. Gali, *Applied Physics Reviews* **7**, 031308 (2020), https://pubs.aip.org/aip/apr/article-pdf/doi/10.1063/5.0006075/14576561/031308_1_online.pdf.
-

Supplementary Information

AB INITIO TREATMENT OF SPIN HAMILTONIAN TENSORS

By means of *ab initio* calculations one may determine the spin Hamiltonian tensors by assuming $|e_\varphi\rangle = \cos(\frac{\varphi}{2})|e_x\rangle - \sin(\frac{\varphi}{2})|e_y\rangle$, where φ is a random rotation angle affected by numerical instabilities. If the Jahn-Teller (JT) adiabatic potential energy surface (APES) exhibits barrier energies then φ is stabilized in one of the three minima: $\varphi = n \times 120^\circ$ where $n = 0, 1, 2$ is an integer. The $\varphi = 60^\circ + n \times 120^\circ$ rotations correspond to saddle points of the APES that separate the minima by barrier energies. One may determine A, D, Q tensors for barrier configurations by restricting the C_{1h} mirror symmetry, thus *ab initio* geometry optimization would not relax to the Jahn-Teller minima.

Now, we determine the non-trivial terms of A, D, Q spin tensors. Here, we will follow the derivation for D but the schema is very similar to either A or Q . If the $|e_x\rangle$ orbital ($\varphi = 0^\circ$) is chosen then $\overleftrightarrow{D}^{(xx)}$ matrix is observed. If $|e_y\rangle$ is chosen at ($\varphi = 180^\circ$) then $\overleftrightarrow{D}^{(yy)}$ is visible. Therefore, *ab initio* calculations may result in different $\overleftrightarrow{D}^{(\varphi)}$ tensors that exhibit terms violating C_{3v} symmetry. We will see that the offdiagonal $\overleftrightarrow{D}^{(xy),(yx)}$ terms are inaccessible by Kohn-Sham density functional theory. However, they are still accessible by means of group theory or evaluation of $\overleftrightarrow{D}^{(\varphi)}$ at intermediate angles. We decompose the zero-field splitting tensor into the following parts by means of Pauli matrices ($\hat{\sigma}_x = \begin{pmatrix} 1 & \\ & 1 \end{pmatrix}$, $\hat{\sigma}_y = \begin{pmatrix} & -i \\ i & \end{pmatrix}$, $\hat{\sigma}_z = \begin{pmatrix} 1 & \\ & -1 \end{pmatrix}$) for orbital degrees of freedom as

$$\begin{aligned} \hat{W} &= \overleftarrow{S} \overleftrightarrow{D}^{(xx)} \overrightarrow{S} |e_x\rangle\langle e_x| + \overleftarrow{S} \overleftrightarrow{D}^{(xy)} \overrightarrow{S} |e_x\rangle\langle e_y| + \overleftarrow{S} \overleftrightarrow{D}^{(yx)} \overrightarrow{S} |e_y\rangle\langle e_x| + \overleftarrow{S} \overleftrightarrow{D}^{(yy)} \overrightarrow{S} |e_y\rangle\langle e_y| = \\ & \overleftarrow{S} \overleftrightarrow{D}^{(xx)} \overrightarrow{S} \frac{(1 + \hat{\sigma}_z)}{2} + \overleftarrow{S} \overleftrightarrow{D}^{(xy)} \overrightarrow{S} \frac{(\hat{\sigma}_x + i\sigma_y)}{2} + \overleftarrow{S} \overleftrightarrow{D}^{(yx)} \overrightarrow{S} \frac{(\hat{\sigma}_x - i\sigma_y)}{2} + \overleftarrow{S} \overleftrightarrow{D}^{(yy)} \overrightarrow{S} \frac{(1 - \hat{\sigma}_z)}{2} = \\ & \underbrace{\overleftarrow{S} \frac{1}{2} [\overleftrightarrow{D}^{(xx)} + \overleftrightarrow{D}^{(yy)}] \overrightarrow{S}}_{1 \text{ transforms as } A_1} + \\ & \underbrace{\overleftarrow{S} \frac{1}{2} [\overleftrightarrow{D}^{(xx)} - \overleftrightarrow{D}^{(yy)}] \overrightarrow{S} \hat{\sigma}_z + \overleftarrow{S} \frac{1}{2} [\overleftrightarrow{D}^{(xy)} + \overleftrightarrow{D}^{(yx)}] \overrightarrow{S} \hat{\sigma}_x}_{\{\hat{\sigma}_z; \hat{\sigma}_x\} \text{ transforms as } E} + \underbrace{\overleftarrow{S} \frac{1}{2} [\overleftrightarrow{D}^{(xy)} - \overleftrightarrow{D}^{(yx)}] \overrightarrow{S} i\hat{\sigma}_y}_{i\hat{\sigma}_y = L_z \text{ transforms as } A_2}, \end{aligned} \quad (\text{S1})$$

where the selected decomposition shows the orbital operator's symmetry. The first symmetrized term will transform as A_1 and thus will contain the D parameter. There are two terms that transform as E : D_1 and D_2 . However, it is worth to note that there will be no terms transforming as A_2 since all tensors are symmetric thus the last term can be neglected.

At the same time we construct the symmetry adapted \hat{W} interaction terms exhibiting \hat{S}_i operators in the second order as

$$\begin{aligned} \hat{W} &= D \left[\hat{S}_z^2 - \frac{1}{3} S(S+1) \right] + \\ & D_1 \left[(\hat{S}_x \hat{S}_z + \hat{S}_z \hat{S}_x) \hat{\sigma}_z + (\hat{S}_y \hat{S}_z + \hat{S}_z \hat{S}_y) \hat{\sigma}_x \right] + \\ & D_2 \left[(\hat{S}_y \hat{S}_y - \hat{S}_x \hat{S}_x) \hat{\sigma}_z + (\hat{S}_x \hat{S}_y + \hat{S}_y \hat{S}_x) \hat{\sigma}_x \right] \end{aligned} \quad (\text{S2})$$

that is equivalent of Eq. (4) of the main text by $\hat{S}_\pm = \hat{S}_x \pm i\hat{S}_y$ and $\hat{\sigma}_\pm = (\hat{\sigma}_x \pm i\hat{\sigma}_y)/2$ transformations. By comparing the similarities of Eqs. (S1) and (S2), and calculating $\langle e_x | \hat{W} | e_x \rangle$ or $\langle e_y | \hat{W} | e_y \rangle$ we arrive at

$$D_1 = D_{xz}^{(xx)} = D_{yz}^{(yy)} \quad \text{and} \quad D_2 = D_{xy}^{(yy)} = (D_{yy}^{(xx)} - D_{xx}^{(xx)})/2, \quad (\text{S3})$$

showing a practical method to evaluate D_1 and D_2 directly from Kohn-Sham density functional theory calculations. We note that arbitrary φ by $\langle e_\varphi | \hat{W} | e_\varphi \rangle$ would result in

$$|D_1| = \sqrt{(D_{xz}^{(\varphi)})^2 + (D_{yz}^{(\varphi)})^2} \quad \text{and} \quad |D_2| = \sqrt{(D_{xy}^{(\varphi)})^2 + \frac{1}{4}(D_{xx}^{(\varphi)} - D_{yy}^{(\varphi)})^2}. \quad (\text{S4})$$

For example, density functional theory calculation at PBE level without symmetry constraints leads to zero-field splitting tensor

$$\overleftrightarrow{D}_{\text{cartesian}}^{(xx)} = \begin{pmatrix} 251 & -575 & 1120 \\ -575 & 251 & 1120 \\ 1120 & 1120 & -503 \end{pmatrix} \text{ MHz} \quad (\text{S5})$$

in the Cartesian coordinates of the diamond lattice. Transformation into the $[111]$, $[2\bar{1}\bar{1}]$, $[01\bar{1}]$ coordinate system of diamond NV center will lead to the following matrices

$$\overleftrightarrow{D}_{\text{DFT}}^{(xx)} = \overleftrightarrow{R}^{-1} \overleftrightarrow{D}_{\text{cartesian}}^{(xx)} \overleftrightarrow{R} = \begin{pmatrix} -\frac{1}{3}D - D_2 & 0 & +D_1 \\ 0 & -\frac{1}{3}D + D_2 & 0 \\ +D_1 & 0 & +\frac{2}{3}D \end{pmatrix} = \begin{pmatrix} -1937 & 0 & -444 \\ 0 & +827 & 0 \\ -444 & 0 & +1110 \end{pmatrix} \text{ MHz}, \quad (\text{S6})$$

that leads to the following *ab initio* zero-field splitting parameters,

$$\begin{aligned} D_{\text{DFT}} &= D_{zz}^{(xx)} - (D_{xx}^{(xx)} + D_{yy}^{(xx)})/2 = +1665 \text{ MHz} \\ D_{1,\text{DFT}} &= D_{xz}^{(xx)} = -444 \text{ MHz} \\ D_{2,\text{DFT}} &= (D_{yy}^{(xx)} - D_{xx}^{(xx)})/2 = +1382 \text{ MHz} \end{aligned} \quad (\text{S7})$$

However, D_1 and D_2 terms will be reduced further by the $q = 0.652$ Ham reduction factor as discussed in the main text as

$$\begin{aligned} D_{\text{theory}} &= D_{\text{DFT}} = +1665 \text{ MHz} \\ D_{1,\text{theory}} &= q \times D_{1,\text{DFT}} = -290 \text{ MHz} \\ D_{2,\text{theory}} &= q \times D_{2,\text{DFT}} = +901 \text{ MHz} \end{aligned} \quad (\text{S8})$$

THEORETICAL NUCLEAR SPIN-FLIP PROBABILITIES

According to nuclear spin-flip probability reported in the Supp. Mat. of Ref. 84 we crudely approximate the flipping probabilities for a saturated $20 \mu\text{s}$ readout sequence. We take the values from Table 2 of the Supp. Mat. and we summed the probabilities for different $m_S = \pm 1$ for the sake of simplicity. We try to use experimental parameters if available but revert to our theoretical values as no experimental data is reported. In Fig. S1(d) of Ref. 84 it is depicted that at $2 \mu\text{W}$ laser power used in the experiments saturated the count rate. We interpret this as whenever the system relaxes back to $|^3A_2\rangle$ it is excited again into the $|^3E\rangle$ manifold with nearly zero waiting time. We use the experimentally observed $\tau_{\text{rad}} = 12.0 \text{ ns}$ radiative lifetime to estimate the length of stay within $|^3E\rangle$ and assume a 0.5 ns waiting time for $|^3A_2\rangle$ as a crude approximation. Therefore, during a $20 \mu\text{s}$ interval there will be $n = 20000/12.5 = 1600$ optical cycles total for a single NV center in diamond.

Firstly, we determine the nuclear spin-flip probabilities by means of $A_{\perp}^{(e)}$. For simplicity, we neglect the strain splitting within $|^3E\rangle$. Our initial state is an $m_S = 0$ either $|E_x\rangle$ or $|E_y\rangle$. Thereby, the probability that the system does not remain within $m_S = 0$ and transferred towards any of $|A_1\rangle$, $|A_2\rangle$, $|E_1\rangle$, $|E_2\rangle$ $m_S = \pm 1$ multiplets will be then as follows

$$\begin{aligned} p(|E_x\rangle \otimes |0\rangle \rightarrow |E_{1,2}\rangle \otimes |\pm 1\rangle) &= 2 \times \left(\frac{A_{\perp}^{(e)}}{\lambda^{(e)} - D^{(e)}} \right)^2 \times n = 0.112, \\ p(|E_x\rangle \otimes |0\rangle \rightarrow |A_1\rangle \otimes |\pm 1\rangle) &= 2 \times \frac{1}{2} \left(\frac{A_{\perp}^{(e)}}{\lambda^{(e)} + D^{(e)} - D_2^{(e)}} \right)^2 \times n = 0.017, \\ p(|E_x\rangle \otimes |0\rangle \rightarrow |A_2\rangle \otimes |\pm 1\rangle) &= 2 \times \frac{1}{2} \left(\frac{A_{\perp}^{(e)}}{\lambda^{(e)} + D^{(e)} - D_2^{(e)}} \right)^2 \times n = 0.021, \end{aligned} \quad (\text{S9})$$

where the $2 \times$ factor corresponds to the photon absorption and luminescence events for each optical cycle. We note that, $Q_1^{(e)}$ corresponds to an additional 0.0073 probability. Therefore, there will be a total $(0.112 + 0.017 + 0.021 + 0.001) = 0.16$ probability to flip the nuclear spin from $|0\rangle$ to $|\pm 1\rangle$. Finally, we note that flipping probabilities from $|\pm 1\rangle$ to $|0\rangle$ are half as much (0.08) because this time there is only one $|0\rangle$ final state instead of two $|\pm 1\rangle$.

On the other hand, we evaluate $Q_2^{(e)}$ by Schrödinger evolution as we discussed in the main text, and arrive at the following result,

$$p(|E_+\rangle \otimes |-1\rangle \rightarrow |E_-\rangle \otimes |+1\rangle) = 4(Q_2^{(e)} n \tau_{\text{rad}})^2 = 0.436, \quad (\text{S10})$$

where $|E_{\pm}\rangle = (|E_x\rangle + i|E_y\rangle)/\sqrt{2}$. Here we also consider that $|E_x\rangle$ and $|E_y\rangle$ sublevels were split by $\delta_{\perp} = 3$ GHz by local strain, see Fig. 1.(a) in Ref.[84] and $|E_y\rangle$ were selectively excited. Therefore, only the $|E_y\rangle \otimes |\pm 1\rangle \rightarrow |E_y\rangle \otimes |\mp 1\rangle$ transition will be available:

$$p(|E_y\rangle \otimes |\mp\rangle \rightarrow |E_y\rangle \otimes |\pm\rangle) = (Q_2^{(e)} n\tau_{\text{rad}})^2 = 0.109, \quad (\text{S11})$$

and the

$$p(|E_y\rangle \otimes |\mp\rangle \rightarrow |E_x\rangle \otimes |\pm\rangle) = 0, \quad (\text{S12})$$

process is quenched by the δ_{\perp} strain.